Simulations of Kink-like Modes in NSTX Plasmas

Ge Dong[1], Mario Podesta[1], Joseph McClenaghan[2], and Zhihong Lin[2]
[1] Princeton Plasma Physics Lab
[2] University of California, Irvine

APS-DPP
Savannah, Georgia
November, 2015

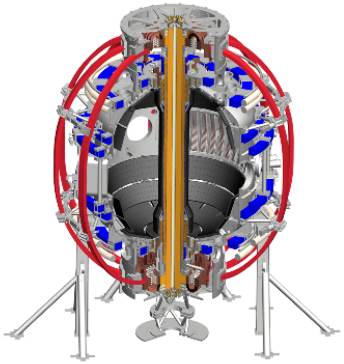

INTRODUCTION

GYROKINETIC SIMULATION MODEL FOR KINETIC MHD

GTC GYROKINETIC SIMULATIONS WITH NSTX EQUILIBRIUM

GYROKINETIC SIMULATIONS WITH FAST IONS

CONCLUSIONS AND FUTURE WORK

Outline

- Introduction
  - Motivations
  - Gyrokinetic simulation model for kinetic MHD
- GTC simulations with NSTX equilibrium
  - Simulations in fluid limit
  - Simulations with kinetic ions
  - Simulations with kinetic ions and fast ions
- Conclusions and future work
  - Linear simulations with various equilibriums
  - Nonlinear gyrokinetic simulations to compare with experimental results

Introduction- Motivation

- Kink-like instabilities destabilized by energetic ions can lead to deterioration of plasma confinement[1]. Therefore understanding their stability properties and dynamics is important to improve the machine performance.
- Thermal ion kinetic effects can play important role on the excitation and evolution of the internal kink modes, as well as other MHD modes. Sufficient fast ion pressure can destabilize non-resonant kink (NRK) modes and fishbone modes through wave particle resonance[2],[3],[4].
- We use gyrokinetic particle simulations to study the kinetic effects of thermal ions and fast ions on kink instabilities in NSTX plasmas, which usually has a large super-Alfvenic fast ion population[5]. This study provides basis for comparison of experimental data and simulation results.

Introduction- Gyrokinetic simulation model for kinetic MHD in GTC

Frequency and growth rate of the kinetic-MHD modes are much smaller than Ω_i, so a gyrokinetic model for the ions is used to study these modes with all the wave-particle resonance and finite Larmor radius effects[6],[7]. In analytical equilibrium the model without kinetic ions is benchmarked with MHD theory[7].

Electron fluid equation from the electron drift kinetic equation to get δn_e

$$\frac{\partial \delta n_e}{\partial t} + \mathbf{B_0} \cdot \nabla \left(\frac{n_0 \delta u_{\|e}}{B_0} \right) + B_0 \mathbf{v_E} \cdot \nabla \left(\frac{n_0}{B_0} \right) - n_0 (\mathbf{v}_* + \mathbf{v_E}) \cdot \frac{\nabla B_0}{B_0}$$
$$+ \delta \mathbf{B}_\perp \nabla \left(\frac{n_0 u_{\|0}}{B_0} \right) + \frac{c \nabla \times \mathbf{B_0}}{B_0^2} \left(-\nabla \delta P_\| + n_0 \nabla \delta \phi \right) = 0$$

where the drift velocities are

$$\mathbf{v_E} = \frac{c \mathbf{b}_0 \times \nabla \delta \phi}{B_0}$$

$$\mathbf{v_{*e}} = \frac{\mathbf{b}_0 \times \nabla \left(\delta P_{\|e} + \delta P_{\perp e} \right)}{n_{0e} B_0}$$

Gyrokinetic poisson equation using Pade approximation to get $\delta\Phi$

$$\frac{c^2}{4\pi v_A^2} \nabla_\perp^2 \delta \phi = -\left(1 - \rho_i^2 \nabla_\perp^2\right) \left(Z_i \overline{\delta n}_i - \delta n_e\right)$$

Gyrokinetic Ampere's law to calculate electron perturbed current

$$n_{0e} e \delta u_{\|e} = \frac{c}{4\pi} \nabla_\perp^2 A_\| + Z_i n_{0i} \overline{\delta u}_{\|i}$$

Where the vector potential is calculated from:

$$\frac{\partial \delta A_\|}{\partial t} = c \mathbf{b}_0 \cdot \nabla \phi_{\text{ind}} \qquad \phi_{\text{ind}} = \phi_{\text{eff}} - \delta \phi$$

$\delta\Phi_{\text{eff}}$ describes parallel electric field (removing tearing mode), to the lowest order:

$$\delta \phi_{eff} = e T_e \frac{\delta n_e}{n_{0e}} - \frac{\delta \psi}{n_{0e}} \frac{\partial n_{0e}}{\partial \psi_0}$$

Ion gyrokinetic equation and gyrocenter equations of motion

The parallel and perpendicular perturbed electron pressures in the lowest order are:

$$\delta P_{\|e} = \delta P_{\perp e} = n_{0e} e \delta\phi_{eff} + \frac{\partial(n_{0e}T_e)}{\partial\psi_0}\delta\psi$$

$\delta\psi$: perturbed poloidal flux
ψ_0 : equilibrium poloidal flux

the ion flow $\mathbf{u_i}$ and the ion density n_i in Poisson's Eq and Ampere's Law are calculated using the gyrokinetic equation

$$\frac{d}{dt}f_i(\mathbf{X},\mu,v_\|,t) \equiv \left[\frac{\partial}{\partial t} + \nabla\cdot\dot{X} + \dot{v}_\|\frac{\partial}{\partial v_\|}\right]f_i = 0.$$

X : position of the gyrocenter
$v_\|$: velocity parallel to the magnetic field
μ : the magnetic moment of the ion

The ion gyrocenter motion is governed by

$$\dot{\mathbf{X}} = v_\|\mathbf{b} + \mathbf{v}_E + \mathbf{v}_d,$$

$$\dot{v}_\| = -\frac{1}{m_i}\frac{\mathbf{B}^*}{B_0}\cdot(\mu\nabla B_0 + Z_i\nabla\delta\phi) - \frac{Z_i}{m_i}\frac{\partial\delta A_\|}{\partial t}$$

where the corrected magnetic field is

$$\mathbf{B}^* = \mathbf{B}_0^* + \delta\boldsymbol{B} = \mathbf{B}_0 + \frac{B_0 v_\|}{\Omega_i}\nabla\times\mathbf{b}_0 + \delta\boldsymbol{B}$$

E×B drift is: $\mathbf{v_E} = \frac{c\mathbf{b}_0\times\nabla\delta\phi}{B_0}$

and magnetic drift velocity v_d is the sum of the curvature drift v_c and grad-B drift v_g

$$\mathbf{v}_d = \mathbf{v}_c + \mathbf{v}_g = \frac{v_\|^2}{\Omega_i}\nabla\times\mathbf{b}_0 + \frac{\mu}{m_i\Omega_i}\mathbf{b}_0\times\nabla B_0$$

Spectrograms of magnetic fluctuations in kink unstable NSTX equilibriums

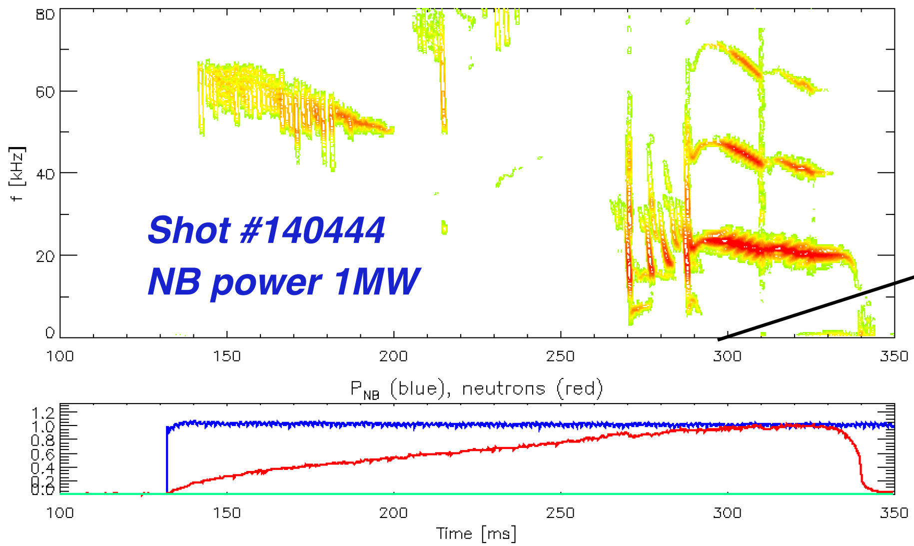

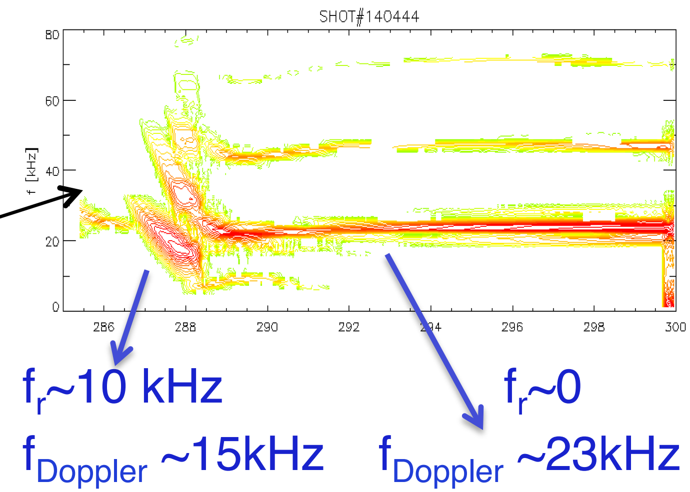

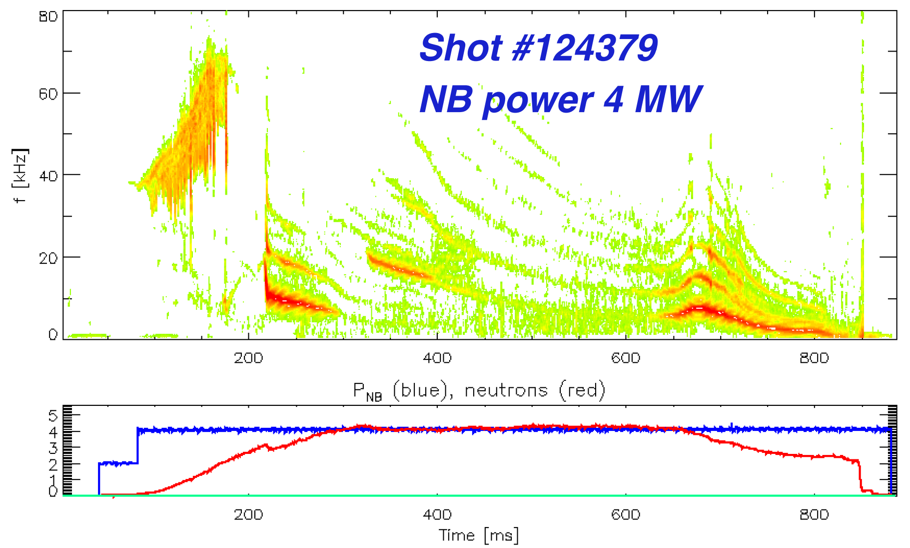

- $f_{measured}=f_r+n\ f_{Doppler}$
- Instabilities have dominant n=1 toroidal component
- Bursting modes with chirping real frequency are identified as fishbone
- Long-lived modes with nearly zero real frequency are identified as NRK.
- In shots with different NB power, transitions from fishbone mode to NRK are observed.

Simulation parameters using NSTX equilibriums

Shot # 124379 at 635 ms using TRANSP[8] result

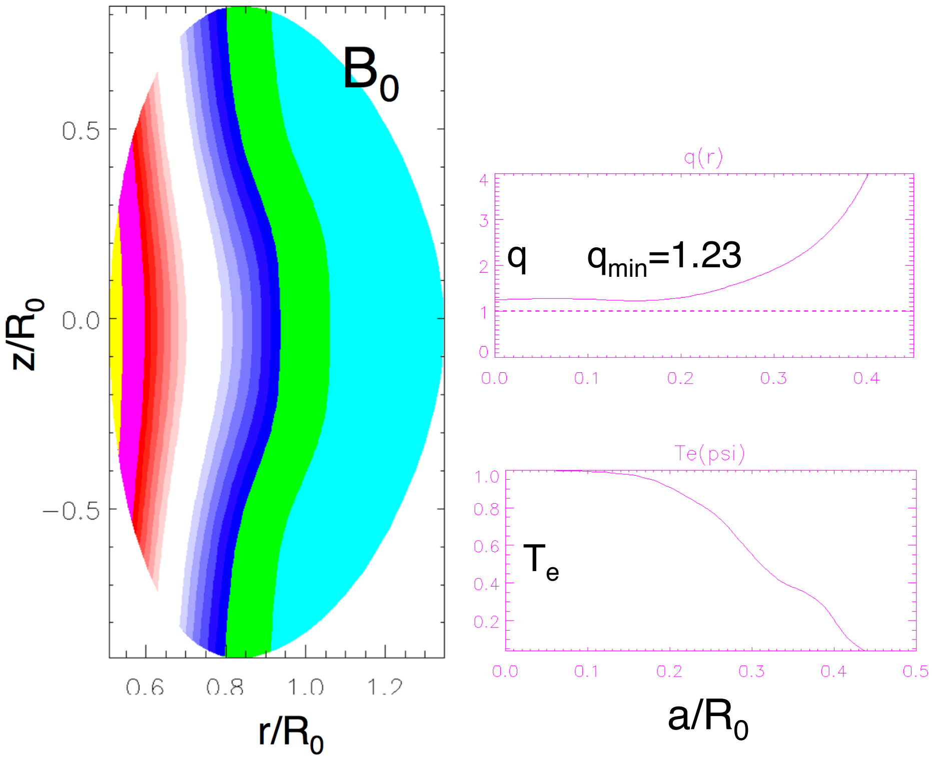

n_e= 9.34×10^{19} m^{-3}

T_e= 0.870 keV *(artificially increased to 2.3keV in fluid simulations to match total beta)*

R_0= 101.83 cm

B_0= 0.454 T

Shot # 140444 at 300 ms

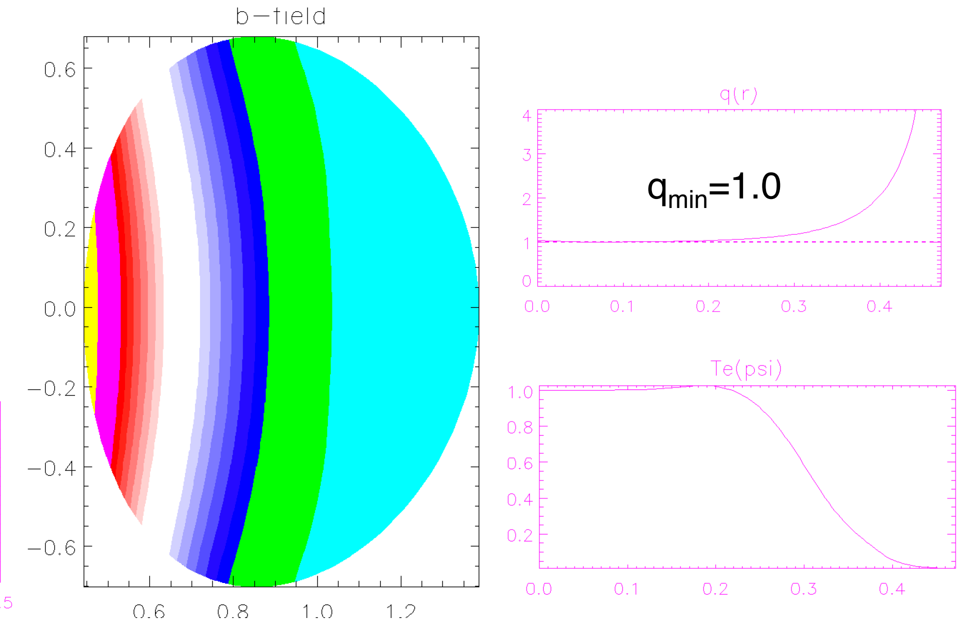

n_e = 3.01×10^{19} m^{-3}

T_e = 3.474 keV *(artificially increased to 4.1keV in fluid simulations to match total beta)*

R_0 = 95.3 cm

B_0 = 0.422 T

Simulation result of NRK in fluid limit

δΦ m=1 component time history

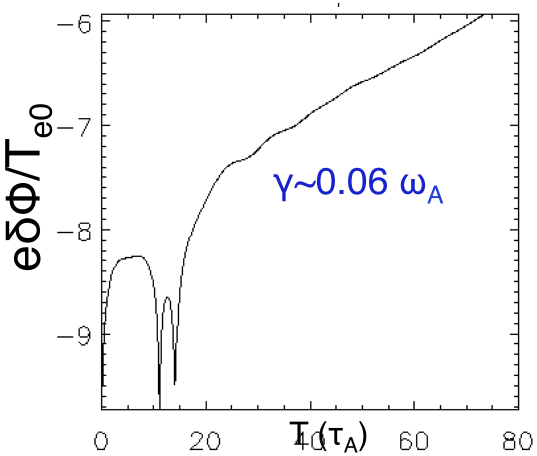

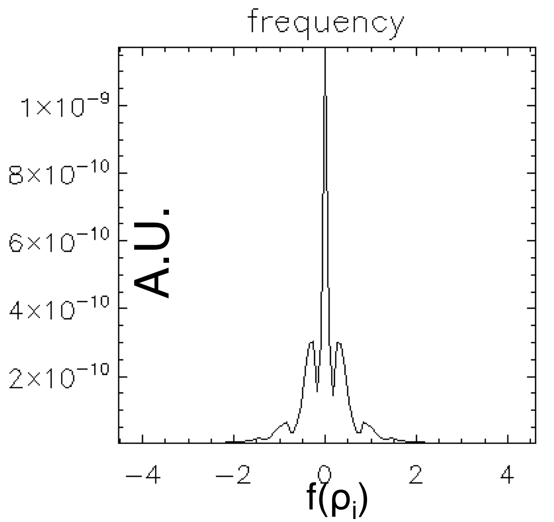

Shot # 124379 at 635 ms

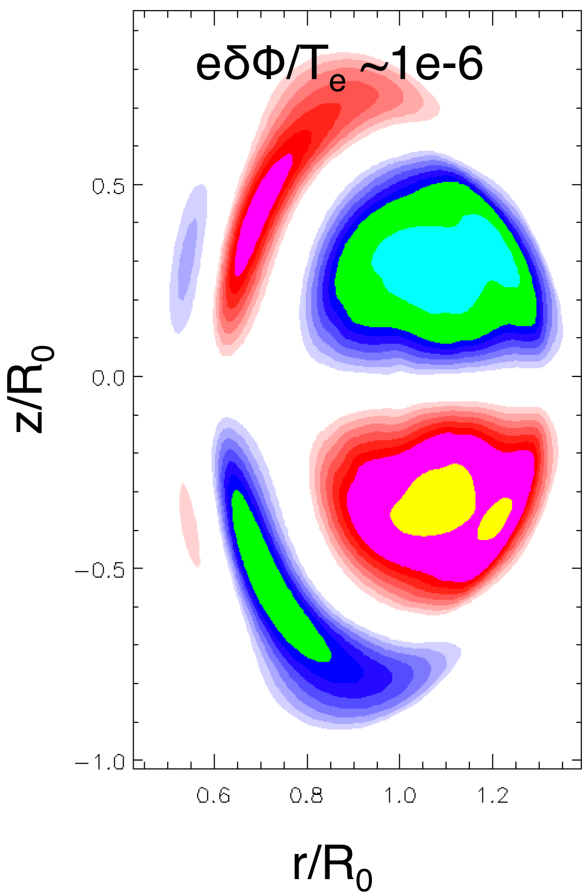

- Using the equilibrium from shot # 124379, in the fluid limit, the mode has a zero real frequency, which is consistent with the MHD model[9].
- There is no q=1 rational surface in this equilibrium. q profile has a reversed shear at r~0.16 R_0, q_{min}=1.23. The mode structure is mainly around the q_{min} surface

A scan of q profile in simulations in fluid limit recovers the experimental regime of kink instability

- In the fluid limit simulations, the ion kinetic effects are suppressed, and the parallel electric field is set to zero ($\delta\Phi_{eff}$=0), therefore the electron β does not enter the equations.

- For the experimental profiles in shot # 124379, a scan of q shows that the mode is unstable for q_{min} <1.4.

- However with smoothened electron temperature and density profile, the mode becomes stable at the measured q profile, with q_{min}=1.23. All other parameters are kept the same.

- This indicates that the mode stability is sensitive to the gradient of the electron pressure.

A modified electron pressure profile will strongly affect the stability of the mode

Shot # 124379

Smoothed profile

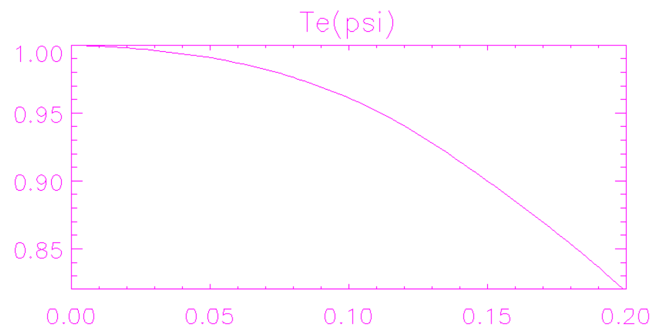

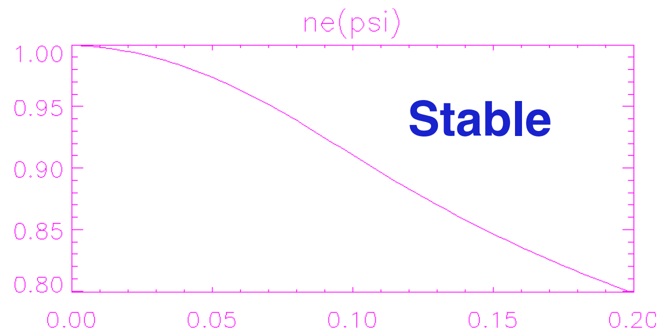

δΦ m=1 component time history

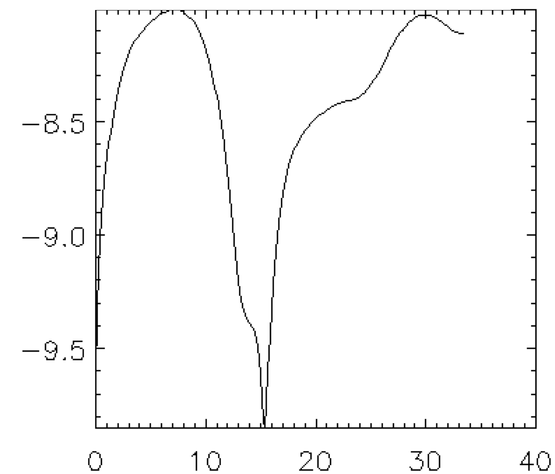

Profile from TRANSP

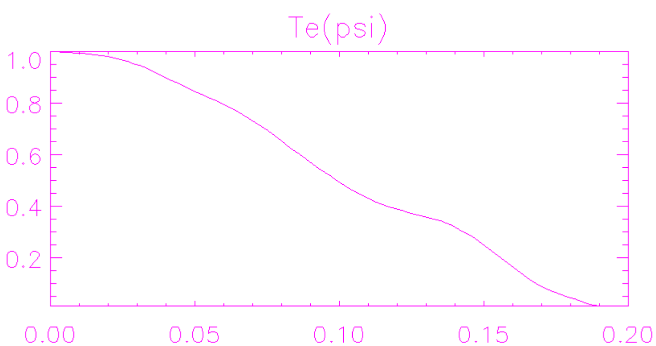

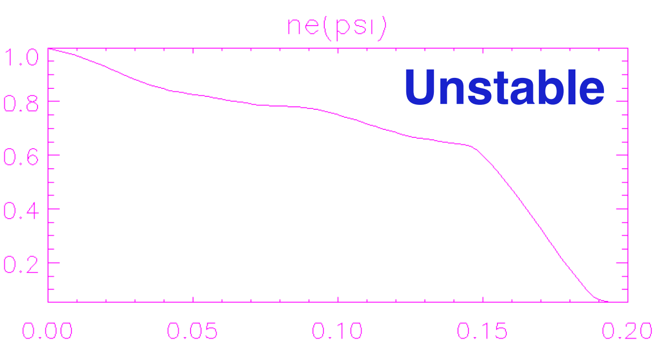

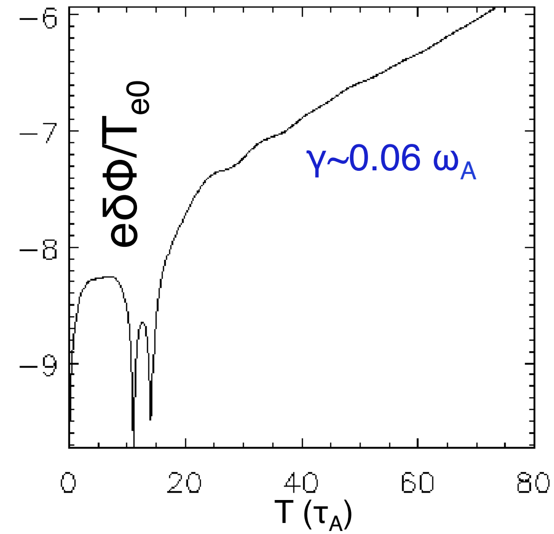

Thermal ion kinetic effects tend to reduce the growth rate of the NRK

Shot # 140444 at 300 ms

Fluid limit

δΦ poloidal structure at linear regime

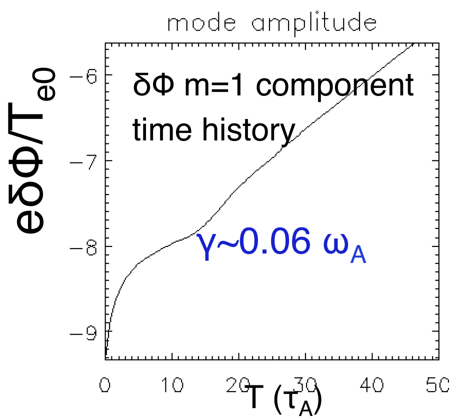

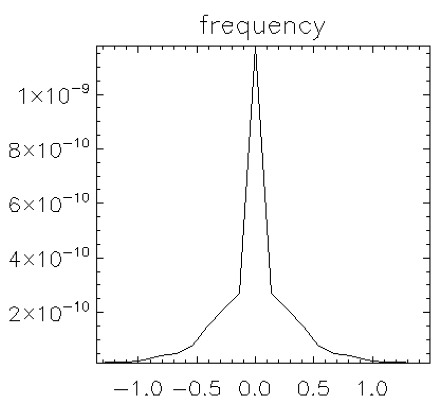

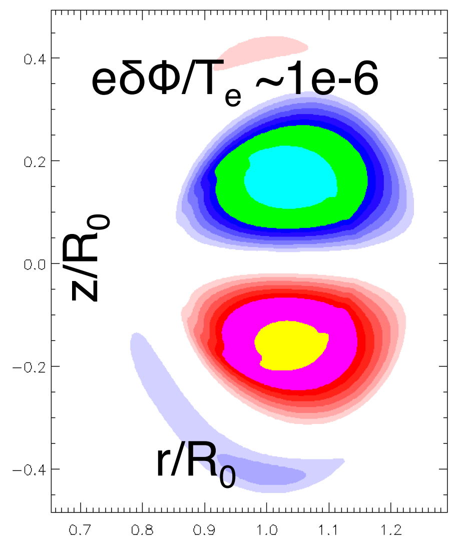

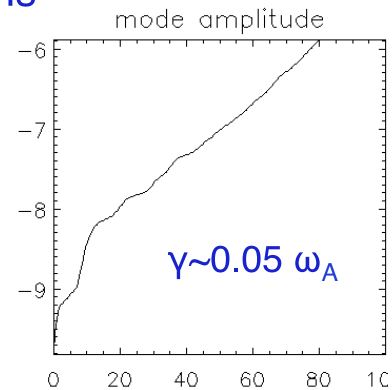

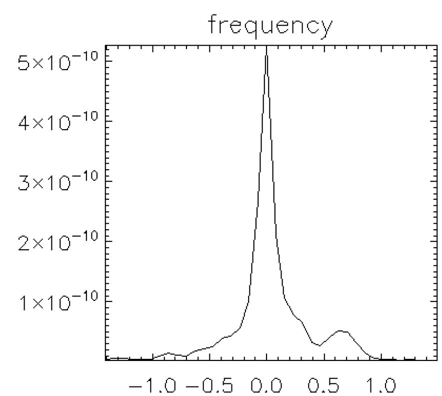

With kinetic ions

δΦ poloidal structure with similar amplitude as in fluid case

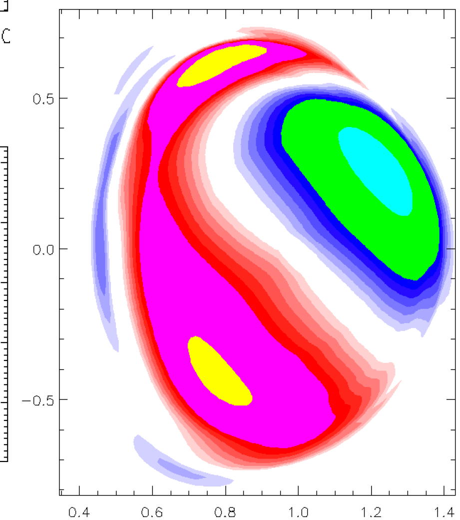

$e\delta\Phi/T_e \sim 1e\text{-}6$

- With the kinetic ions, the real frequency of the mode remains zero, and growth rate slightly decreased.
- The mode structure is slightly modified.

With fast ions EP driven modes with finite real frequency can become dominant over NRK

- The fast ion results are still preliminary. In the linear regime, the mode has a larger growth rate than in the cases without fast ions.
- Real frequency of the mode is within the physical regime of a fishbone mode.
- Precesisonal frequency of the fast ion is f_{pre} ~20 kHz

With fast ions

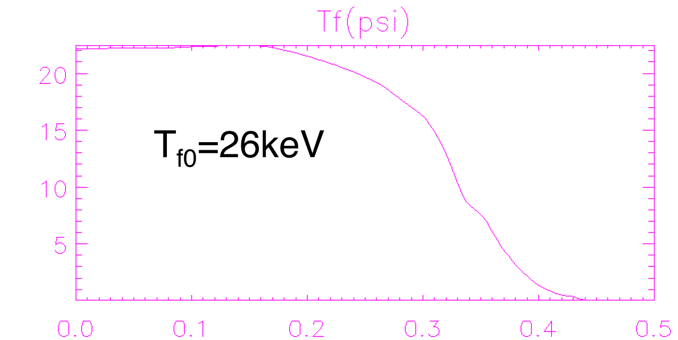

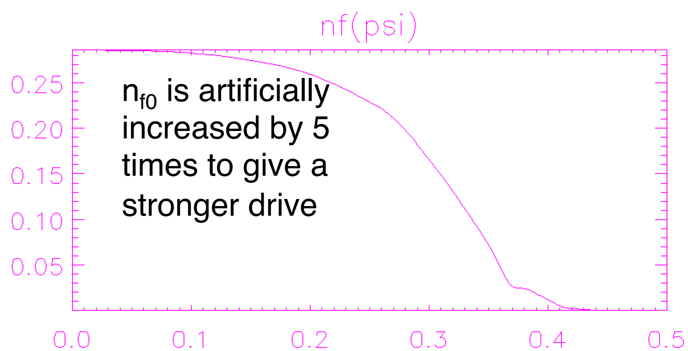

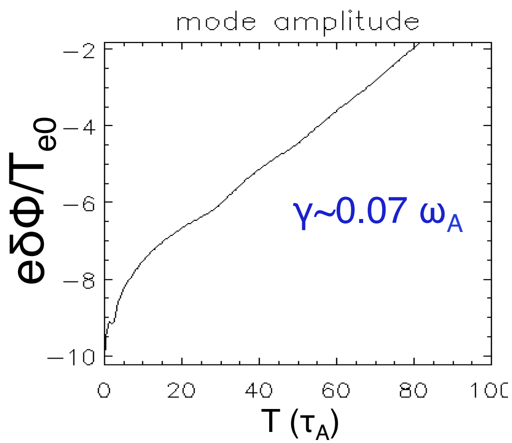

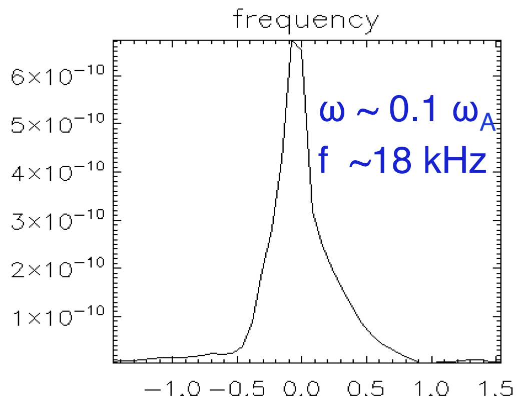

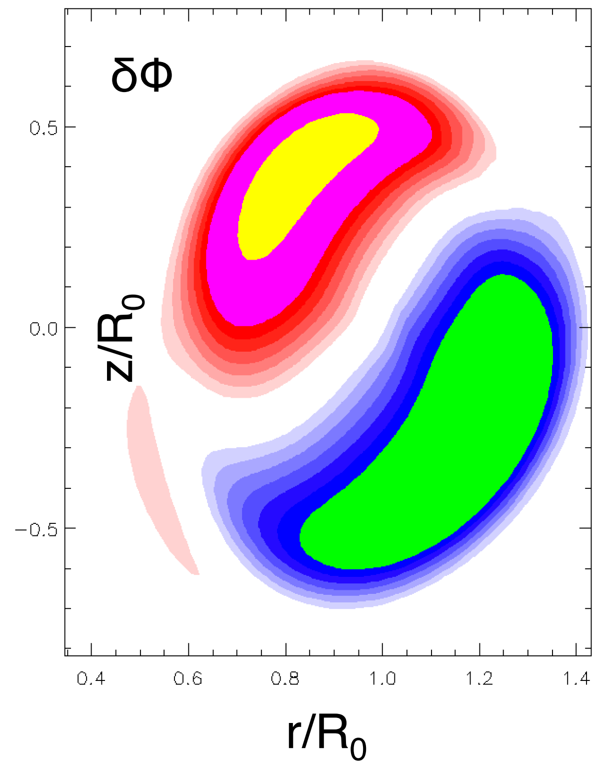

Conclusions

- In fluid limit with experimental plasma density and temperature profiles, a scan of the q profile shows the NRK remains unstable for up to q_{min} ~1.4. A reduced electron temperature or smoothing of the density and temperature profile will make the stability threshold in q_{min} lower.
- The growth rate of the NRK are slightly reduced in simulations with kinetic thermal ions. The mode structures can also be affected.
- In simulations with sufficient fast ion pressure, a fishbone modes with finite real frequency and rotating mode structure can be destabilized.

Future work: Comparison with experimental data base

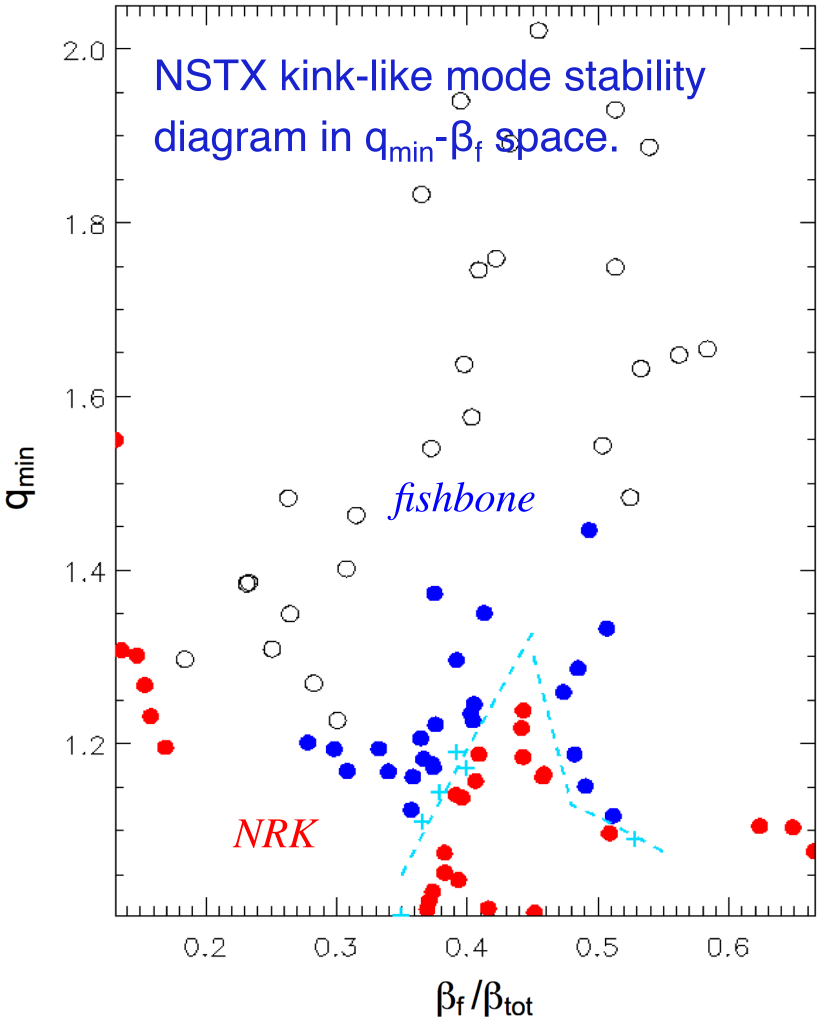

- An experimental characterization of kink-like modes for different NBI scenarios and fast ion properties in NSTX plasmas is available for comparison with simulation results.
- The transition from fishbone to NRK at large electron β can be studied numerically using different experimental equilibrium profiles.

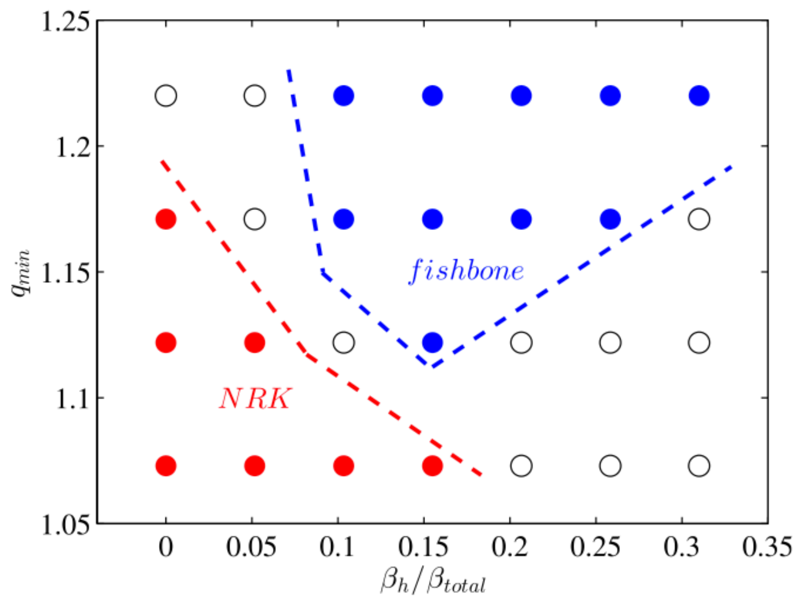

NRK/fishbone stability diagram from M3D-K simulations
Phys. Plasmas 20, 102506 (2013) [10]

Future work: Comparison of non-linear simulation results with kink-like modes diagnostic database on NSTX

- Finite element method field solver in GTC is being developed to resolve the numerical issues associated with the magnetic axis, so that the code can use as input equilibriums with more complex magnetic field geometry. Then kink linear stability properties in more experimental equilibrium with different NB scenarios can be studied in the simulations.
- In longer runs with non-linear terms, mode saturation with frequency/growth-rate evolution and transport properties can be studied and compared with the experimental measurements.

This work is partly supported by US-DoE contract DE-AC02- 09CH11466

Reference

[1] M. Ono, et. al., Nucl. Fusion **40**, 557 (2000).

[2] L. Chen, R. B. White and M. N. Rosenbluth, Phys. Rev. Lett. **52**, 1122-1125 (1984).

[3] E. Frederickson, L. Chen, and R. B. White, Nucl. Fusion **43**, 1258-1264 (2003).

[4] M. N. Bussac, et. al., Phys. Rev. Lett. **35**, 1638 (1975).

[5] M. Podesta, et. al., Nucl. Fusion **51**, 063035 (2011).

[6] I. Holod, et. al. Phys. Plasmas **16**, 122307 (2009).

[7] J. McClenaghan, et. al., Phys. Plasmas **21**, 122519 (2014).

[8] R. J. Goldston *et al.*, J. Comput. Phys. **43**, 61 (1981)

[9] M. N. Rosenbluth, R. Y. Dagazian, and P. H. Rutherford, Phys. Fluids 16(11), 1894–1902 (1973)

[10] F. Wang, *et al.*, Phys. Plasmas **20**, 102506 (2013)